



MSX Infrared Dark Clouds in the BU-FCRAO Galactic Ring Survey: A Galactic Ring Population



R. Simon, R. Y. Shah, J. M. Jackson, T. M. Bania, D. P. Clemens, & M. H. Heyer¹

Institute for Astrophysical Research, Boston University, ¹Five College Radio Astronomy Observatory, University of Massachusetts, Amherst

Abstract

Recent high resolution surveys with the *ISO* and *MSX* satellites have revealed a large number of Galactic clouds with significant extinction in the mid-infrared. The infrared dark clouds are characterized by their high column densities and low temperatures. Little is known, however, about their origin and distribution in the Galaxy.

The BU-FCRAO Galactic Ring Survey (GRS), a high resolution survey of ¹³CO emission in the inner Milky Way, makes it possible to derive physical parameters of IR dark clouds and their parental molecular clouds, such as sizes and masses, by spectroscopically determining their kinematic distances. Based on morphological correlation of IR extinction and GRS ¹³CO emission in velocity channel maps, we assign radial velocities to the IR dark clouds throughout the first Galactic quadrant and, assuming they are at the near kinematic distance, determine their location in the Galaxy. We find that the majority of the IR dark clouds are concentrated in the Galactic Ring at a Galactocentric radius of 5 kpc. We suggest that the most massive IR dark clouds represent high mass proto-clusters, or OB-associations in the making.

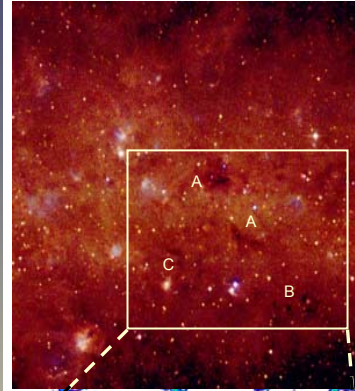
GRS and MSX datasets

The Milky Way Galactic Ring Survey (*GRS*), described in poster # 122.22 (Shah et al. 2003) is designed to probe the star-forming and quiescent molecular gas comprising the 5 kpc Galactic Ring.

The Midcourse Space Experiment (*MSX*) surveyed the entire Galactic plane within $|b| \leq 5^\circ$ in four mid-infrared spectral bands between 6 and 25 μm (Price et al. 2001, AJ 121, 2819).

Survey	Wavelength	Coverage	Ang. Res. / Grid	
GRS	3 mm	ℓ : 18° to 52° b : -1° to $+1^\circ$	$46''/22''$	Spectral Res.: 0.25 km s^{-1} Sensitivity: 0.4 K
MSX Band	A: 6.8-10.8 μm	ℓ : whole plane b : -5° to $+5^\circ$	$20''/6''$	Most sensitive Band, PAH
	C: 11.1-13.2 μm			
	D: 13.5-15.9 μm			
	E: 18.2-25.1 μm			

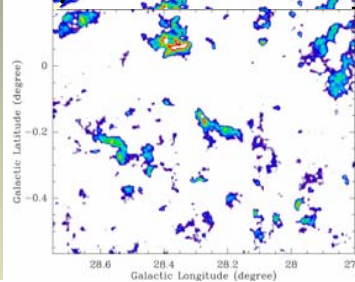
Dark cloud identification



Left: MSX 3-color image of a 1.5×1.5 degree field in the Galactic plane centered at $\ell=28$, $b=0$ degrees. The color coding of the MSX bands in this image is (R, G, B)=(A, C+D, E), corresponding to central wavelengths of (8, 12+15, 21) μm . A number of infrared dark clouds can easily be identified against the bright background of the Galactic plane. To identify the IR dark clouds throughout the Galactic plane, we use the Band A images, since they have the highest sensitivity and the brightest background.

MSX Band A image I_{ij}
↓ Median Filter
Background image B_{ij}

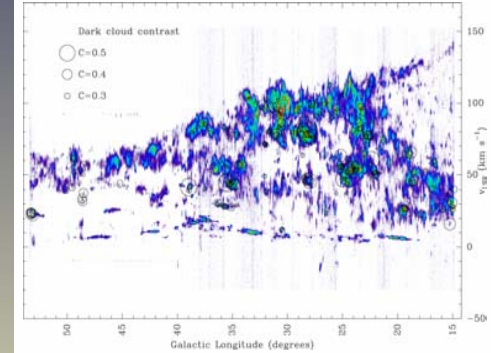
↓
Contrast image $C_{ij} = (B_{ij} - I_{ij})/B_{ij}$



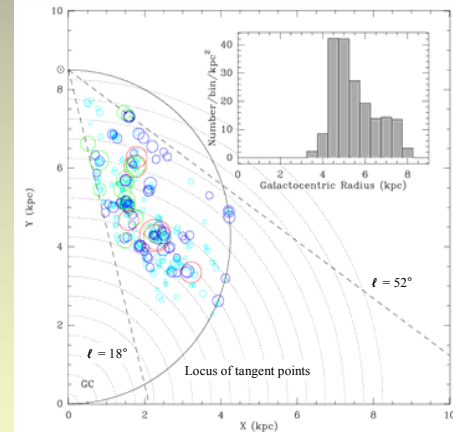
Left: Dark cloud contrast image obtained from the data and the background image. The minimum and maximum contrasts in the image are 0.05 and 0.65, respectively. We selected a total of 375 dark clouds in the current *GRS* coverage with contrasts higher than 20% and sizes greater than 2×2 *MSX* resolution elements. We determine velocities based on morphological correspondence of IR extinction and CO emission in channel maps.

Distances and distribution

Out of the 375 dark clouds selected, 318 have clean morphological matches with *GRS* molecular line emission in distinct velocity channels. The remaining dark clouds are either low contrast clouds, have only weak *GRS* emission counterparts or molecular line emission in more than one velocity channel, or no *GRS* emission at any velocity. The latter are often found close to bright H II regions and are probably holes in the *MSX* emission. To convert the assigned radial velocities into distances, we assume a flat rotation curve with (R_0 , θ_0)=(8.5 kpc, 220 km s^{-1}) and that the dark clouds are located at the near kinematic distance.



The *GRS* l - v diagram from $b=-1^\circ$ to 0.5° . The l - v positions of identified IRDCs are plotted as circles. The sizes of the circles refer to the approximate contrast value found for a given object. Higher contrast means larger Σ_{opt} opacity.



Galactic face-on distribution of the IR dark clouds. The sizes and colors of the symbols represent different contrast ranges:

- $0.2 < C < 0.3$
- $0.3 < C < 0.4$
- $0.4 < C < 0.5$
- $C > 0.5$

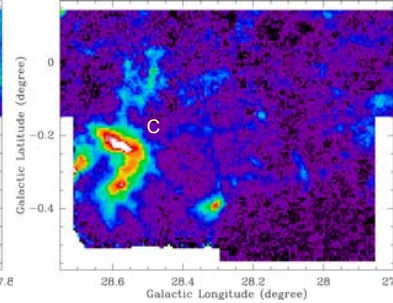
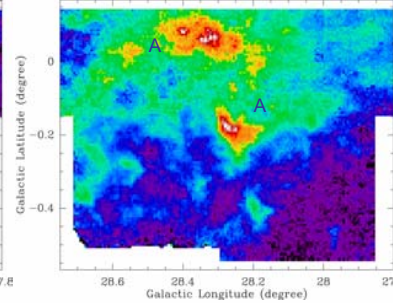
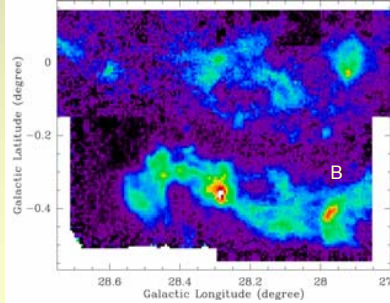
The histogram shows the number distribution of IR dark clouds with Galactocentric radius, weighted by the area of the corresponding face-on segment.

Association with molecular line GRS data

A: $v_{\text{LSR}} 45$ to 50 km s^{-1}

B: $v_{\text{LSR}} 75$ to 80 km s^{-1}

C: $v_{\text{LSR}} 85$ to 90 km s^{-1}



For more information and available data, visit the *GRS* web page at www.bu.edu/GRS
The *MSX* data are available at irsa.ipac.caltech.edu/applications/MSX/

Acknowledgements

The *GRS* acknowledges support from the National Science Foundation via grants AST-9800334 and AST-0098562 and NASA LTSA grant NAG5-10808.

Processing of the *MSX* data was funded by the Ballistic Missile Defense Organization with additional support from NASA Office of Space Science.

- We identified dark regions in the *MSX* survey with the *GRS* ¹³CO survey, assigning radial velocities based on morphological matches. We identify these as infrared dark clouds, or IRDCs.
- Assuming a flat rotation curve and that identification of ¹³CO emission with mid-IR absorption implies nearby heliocentric distances, we produce a face-on plot of the distribution of IRDCs. The associated histogram of number of IRDCs with galactocentric distance shows an enhancement towards the 5 kpc ring.
- The heliocentric distances yield sizes and masses. High contrast IRDCs almost always have bright, extended ¹³CO emission. The masses of the highest contrast dark clouds are typically a few $1000 M_{\text{sun}}$. We suggest that these are the high-mass pre-cursors of OB-associations in the making.

References

Egan et al. 1998, ApJ, 494, L199
Hennebelle et al. 2001, A&A, 365, 598
Sanders et al. 1986, ApJS, 60, 1